Soluble Phosphatidylserine Binds to a Single Identified Site in the C2 Domain of Human Factor V_a[†]

Arvind Srivastava,[‡] M. A. Quinn-Allen,[§] S. W. Kim,[§] W. H. Kane,[§] and B. R. Lentz*,[‡]

Department of Biochemistry and Biophysics, Program in Molecular and Cellular Biophysics, University of North Carolina, Chapel Hill, North Carolina 27599, and Departments of Medicine and Pathology, Duke University Medical Center, Durham, North Carolina 27510

Received March 6, 2001; Revised Manuscript Received May 15, 2001

ABSTRACT: Factor V_a (FV_a) is a cofactor for the serine protease factor X_a that activates prothrombin to thrombin in the presence of Ca^{2+} and a membrane surface. FV_a is a heterodimer composed of one heavy chain (A1 and A2 domains) and one light chain (A3, C1, and C2 domains). We use fluorescence, circular dichroism, and equilibrium dialysis to demonstrate that (1) the FV C2 domain expressed in Sf9 cells binds one molecule of C6PS with a k_d of ~2 μM, (2) stabilizing changes occur in the FV C2 domain upon C6PS binding, (3) the C6PS binding site in the FV C2 domain is located near residue Cys^{2113}, which reacts with DTNB, and (4) binding to a PS-containing membrane is an order of magnitude tighter than that to soluble C6PS. Coupled with a recently published crystal structure of the C2 domain, these results support a model for the mechanism of C2−membrane interaction.

Blood coagulation factor V_a is an essential component of the prothrombinase complex, which consists of serine protease factor X_a, cofactor factor V_a, Ca^{2+}, and a phospholipid membrane (*16*, *29*, *40*). The prothrombinase complex catalyzes the rapid conversion of prothrombin to thrombin, which is a crucial step in normal hemostasis (*7*, *29*). Factor V exists in plasma as an inactive, large, single-chain glycoprotein with little or no intrinsic procoagulant activity (*6*, *31*). It is composed of repeating domains: two A domains at the amino-terminal end, a heavily glycosylated connecting B domain, a third A domain, and two carboxyl-terminal C domains (*12*, *15*, *17*). Limiting proteolysis of factor V by thrombin (*6*, *18*), factor X_a (*30*), or the factor V activator from Russell's viper venom (RVV-V) (*18*) results in the expression of procoagulant activity. Thrombin-activated factor V_a is a heterodimer (*8*) composed of a heavy chain (M_r = 94 000; M_r = 105 000 in human) and a light chain (M_r = 74 000 or 71 000) (*6*, *18*). Heterogeneity of the light chain is seen in both bovine and human factor V_a (*6*, *18*, *36*) and is due to alternative glycosylation at Asp^{2181} in the C2 domain (*19*, *32*).

Factor V_a binds to a phosphatidylserine (PS[1])-containing membrane with a k_d of 3 nM (*25*). Early studies suggested that membrane binding was mediated solely by the light chain (*10*), although more recent evidence points as well to interaction of the heavy chain with PS-containing membranes (*23*). An analysis of binding to membranes of varying PS content suggested that factor V_a binds two to four PS molecules (*5*). Putative phospholipid binding sites have been identified in both the A3 (*14*) and C2 (*36*) domains of factor V. However, recent molecular modeling studies have suggested that the phospholipid binding to the A3 domain may not be physiological (*42*).

Several lines of evidence suggest that the second C-type domains of factor V and the homologous cofactor factor VIII contain PS-binding sites that are essential for assembly of the functional procoagulant complex (*35*). First, deletion of the C2 domain of factor V results in the loss of both its procoagulant activity and its ability to bind a PS membrane (*35*). Second, naturally occurring immunoglobulins that bind to the C2 domain of factor VIII (*1*) and of factor V (*35*) block binding to PS-containing membranes and inhibit procoagulant activity. Third, the crystal structures of the factor V (*28*) and factor VIII C2 (*38*) domains suggest that membrane binding is mediated by insertion of hydrophobic amino acid side chains into the hydrophobic core of the membrane bilayer and by specific interactions between polar amino acid side chains and the PS headgroup. Finally, we have recently shown that two hydrophobic amino acid sides chains in the C2 domain, Trp^{2063} and Trp^{2064}, are required for high-affinity binding to membranes containing phosphatidylserine. These hydrophobic amino acid side chains are also required for binding to monoclonal antibodies that block factor V binding to phosphatidylserine (*20*). The direct

[†] Supported by Grants HL45916 (B.R.L.) and HL43106 (W.H.K.) from the U.S. Public Health Service.

* To whom correspondence should be addressed. Telephone: (919) 966-5384. Fax: (919) 966-2852. E-mail: uncbrl@med.unc.edu.

[‡] University of North Carolina.

[§] Duke University Medical Center.

[1] Abbreviations: rHFV-C2, C2 domain of human factor V_a; $rHFV_1$-C2, glycosylated C2 domain of human factor V_a; $rHFV_2$-C2, nonglycosylated C2 domain of human factor V_a; C6PS, 1,2-dicaproyl-*sn*-glycero-3-phospho-L-serine; C6PC, 1,2-dicaproyl-*sn*-glycero-3-phosphocholine; C6PG, 1,2-dicaproyl-*sn*-glycero-3-phospho-*rac*-1-glycerol; PS, phosphatidylserine; PC, phosphatidylcholine; PG, phosphatidylglycerol; DOPS, 1,2-dioleoyl-*sn*-glycero-3-phospho-L-serine; DOPC, 1,2-dioleoyl-*sn*-glycero-3-phosphocholine; DOPG, 1,2-dioleoyl-*sn*-glycero-3-phosphoglycerol; DTNB, 5,5-dithiobis(2-nitrobenzoate); SUV, small unilamillar vesicles; ELISA, enzyme-linked immunosorbent assay; CD, circular dichroism; SDS−PAGE, sodium dodecyl sulfate−polyacrylamide gel electrophoresis; CMC, critical micelle concentration.

10.1021/bi010449k CCC: $20.00
Published on Web 06/23/2001

interaction between the factor V C2 domain and phospholipid membranes has not been previously characterized. In this paper, we have expressed the factor V C2 domain (rHFV-C2) in insect cells and have determined the affinity and stoichiometry for binding to membrane and soluble phospholipids.

MATERIALS AND METHODS

Materials

1,2-Dicaproyl-*sn*-glycero-3-phospho-L-serine (C6PS), 1,2-dicaproyl-*sn*-glycero-3-phosphocholine (C6PC), 1,2-dicaproyl-*sn*-glycero-3-phospho-*rac*-1-glycerol (C6PG), 1,2-dioleoyl-*sn*-glycero-3-phospho-L-serine (DOPS), 1,2-dioleoyl-*sn*-glycero-3-phosphocholine (DOPC), 1,2-dioleoyl-*sn*-glycero-3-phosphoglycerol (DOPG), brain phosphatidylserine, and brain phosphatidylcholine were purchased from Avanti Polar Lipids Inc. (Alabaster, AL). Monoclonal antibody 6A5 was generated in our laboratory and was biotinylated as previously described (*34*). Monoclonal antibody HV-1 and DTNB were obtained from Sigma (St. Louis, MO). All other chemicals were American Chemical Society (ACS) reagent grade or the best available grade.

Methods

Preparation of Soluble C6PS, C6PG, and C6PC. C6PS, C6PG, and C6PC solutions were prepared from measured quantities of 10 mg/mL stock solutions in chloroform. The chloroform was evaporated under a stream of nitrogen. The lipid was redissolved in cyclohexane, and then the shell frozen solution was lyophilized overnight to a white powder. The resulting dry powder was dispersed in the appropriate volume of buffer and vortexed thoroughly to reach a concentration of approximately 2 mM. The final concentration of the phospholipid stock solutions was determined by an inorganic phosphate assay (*3*).

Preparation of Small Unilamellar Vesicles. Small unilamellar vesicles (SUV) composed of 80:20 (mole ratio) of DOPC/DOPS and DOPC/DOPG mixtures and pure DOPC were prepared by subjecting a multilamellar vesicle suspension to sonic disruption in a Heat System (Plainview, NY) model 350 sonicator (*26*). SUV preparations were fractionated by centrifugation at 70 000 rpm for 25 min in a Beckman (Palo Alto, CA) TL-100 ultracentrifuge. Phospholipid concentrations were determined by the analysis of inorganic phosphate (*3*). SUV were used the same day of preparation.

Insect Cell Expression. The C2 domain of human factor V was amplified by PCR using the factor V cDNA as a template and the primers 5′-CACACATCGATAGCTAGCCATGTTCCCAGGCTGCCCACGCCTC-3′ and 5′-CACAGTCGACAGCTAGCTAGTAAATATCACAGCCAAAGAGT-3′. The amplified fragment was subcloned into pBluescript (Life Technologies, Rockville, MD) for DNA sequencing and restriction mapping. The cDNA insert was then excised using *Nhe*I and subcloned into the expression vector pBluebac II (Invitrogen, Carlsbad, CA). The pBluebac II rHFV-C2 expression plasmid was cotransfected with linearized wild-type *Autographa californica* nuclear polyhedrosis virus (AcMNPV) DNA into *Spodoptera frugiperda* cells (Sf9) using the MaxBac Expression System (Invitrogen). The recombinant virus was plaque purified, and a high-titer stock was prepared using the protocols outlined by the manufacturer. *Trichnoplusia ni* (Hi5) cells were grown in suspension culture using Excell 401 serum free medium (JRH Biosciences, Lenexa, KS) and infected with the recombinant virus using an MOI of 5. The conditioned medium was collected 7 days following infection. Cells were removed by centrifugation, and the conditioned medium was stored at −80 °C until purification. Levels of rHFV-C2 expression were determined by an ELISA using monoclonal antibodies 6A5 and HV-1 as previously described (*36*).

Isolation of rHFV-C2. One liter of conditioned medium containing rHFV-C2 was thawed at 37 °C and centrifuged at 6000*g* for 15 min, sterile filtered, and then degassed for 15 min on ice. All subsequent steps were carried out at 4 °C. The medium was then applied to an SP Sepharose Fast Flow XK 26/40 column (Amersham Pharmacia Biotech Inc., Piscataway, NJ) equilibrated with 5 mM $CaCl_2$, 50 mM NH_4Cl, and 25 mM HEPES (pH 8.0) at a flow rate of 3 mL/min. The column was then washed with 1 L of equilibration buffer and eluted with a 250 mL linear NH_4Cl gradient (from 50 to 1000 mM), collecting 3 mL fractions. Fractions 50−75, which contained rHFV-C2, were pooled and concentrated to a final volume of 10 mL using an Amicon stirred cell concentrator and a YM-1 membrane (Millipore, Bedford, MA). The concentrate was then diluted 5-fold in equilibration buffer and applied to a Mono S column (Amersham Pharmacia Biotech Inc.) using a 50 mL Superloop at a flow rate of 0.5 mL/min. The column was washed with 10 mL of equilibration buffer and then eluted with a 15 mL linear NH_4Cl gradient (from 50 to 1000 mM). To remove minor contaminants that were present in some preparations, selected rHFV-C2 preparations were rechromatographed on the Mono S column in the presence of 5% betaine to minimize nonspecific protein interactions. In the presence of 5% betaine, rHFV-C2 eluted at 650 mM NH_4Cl. The concentration of purified rHFV-C2 was estimated using the extinction coefficient of 2.85 OD/mg that was calculated on the basis of the predicted amino acid composition of rHFV-C2 (*9*).

Sequence and Amino Acid Analysis. Recombinant proteins were first dialyzed against 0.1% trifluoroacetic acid and 10 mM ammonium bicarbonate. Sequence analysis was performed with an Applied Biosystems 477A pulsed liquid-phase sequencer with on-line phenylthiohydantoin analysis using an Applied Biosystems 120A high-pressure liquid chromatography system operated according to the manufacturer's recommendations.

MALDI Mass Spectrometry. MALDI mass spectrometry was carried out by R. Marshall Pope at the mass spectrometry laboratory at the University of North Carolina School of Medicine. Samples were dialyzed into 20 mM ammonium acetate (pH 6.1) prior to analysis.

Titration of Sulfhydryls. The concentration of accessible sulfhydryls was determined under native or denaturing conditions with 5,5′-dithiobis(2-nitrobenzoid acid) (DTNB). For continuous titrations, sample cuvettes contained 8.1 mM C2 domain in 25 mM Hepes, 50 mM NH_4Cl, and 5 mM $CaCl_2$ (pH 7.4) either without denaturant for the determination of the number of accessible sulfhydryl groups in the native conformation or with 8 M urea for the determination of total sulfhydryl content. Sulfhydryl modification was initiated by the addition of DTNB (1.7 mM) to the sample

cuvette, and the formation of 5-thionitrobenzoate was followed continuously by the increase in absorbance at 412 nm. The same solution without the protein was used to assess the spontaneous breakdown of the reagent for subsequent correction of the value determined in the titration the protein. Absorbance readings were converted to molar concentrations of sulfhydryls modified using a molar extinction coefficient of 14 000 at this wavelength.

Solid-Phase ELISA. The solid-phase ELISA was used to detect the effect of HV-1 antibody and DTNB on binding of rHFV-C2 to immobilized phospholipids. Brain phosphatidylserine or phosphatidylcholine was dissolved in methanol to a final concentration of 2 μg/mL, and 100 μL aliquots were added to each well of a 96-well microtiter plate. The wells were allowed to air-dry at room temperature overnight. The wells were blocked with 200 μL of 5 mg/mL gelatin in 0.05 M Tris-HCl and 0.15 M NaCl (pH 7.2) (blocking buffer) for 1 h at 37 °C. The wells were then washed three times with 0.01 M phosphate buffer, 0.12 M NaCl, and 2.7 mM KCl (pH 7.4) with 0.05% (v/v) Tween 20 (washing buffer), and 50 μL samples of the C2 domain were added to each well. After 1 h at 37 °C, the wells were washed three times with washing buffer, and rHFV-C2 binding was detected by using the biotinylated monoclonal antibody 6A5. To determine the effect of monoclonal antibody HV-1 on the binding of rHFV-C2 to phospholipids, rHFV-C2 was incubated with HV-1 for 30 min at 37 °C prior to incubation in the phospholipid-coated wells. To determine the effect of DTNB on the binding of the C2 domain to phospholipids, rHFV-C2 was modified with DTNB and dialyzed prior to incubation in the phospholipid-coated wells.

Determination of the Critical Micelle Concentration (CMC). The diameters of C6PS aggregates were measured by quasi-elastic light scattering, as described previously (*27*). Increasing concentrations of C6PS were added to the sample cell, a 6 mm × 50 mm borosilicate glass disposable culture tube (Baxter Healthcare Corp., McGraw Park, IL), containing 0.4 mL of 0.2 μM rHFV$_2$-C2 in 20 mM KH_2PO_4 and 100 mM NaF (pH 7.4). All buffer solutions were filtered through a 0.8 μm polycarbonate filter (white AAWP, 47 mm, Millipore Corp., Bedford, MA) to decrease the degree of light scattering. The sizes of the various aggregates were measured as intensity-weighted diameters, which were calculated from the *Z*-averaged diffusion coefficient.

Fluorescence Measurements. Intrinsic fluorescence intensity was recorded with an SLM 48000-MHF spectrophotometer (SLM Aminco, Urbana, IL). The excitation wavelength was 285 nm (band-pass at 4 nm), and the emission intensity was recorded at 340 nm (band-pass at 4 nm). Slits were kept closed except during the measurements to avoid photodegradation of the sample. All buffer solutions were filtered through a 0.8 μm polycarbonate filter (white AAWP, 47 mm, Millipore Corp.) to decrease the degree of light scattering. All measurements were carried out at 24 °C. Samples containing 0.2 μM rHFV-C2 in 20 mM KH_2PO_4 and 100 mM NaF (pH 7.4) were titrated with soluble and membrane lipids. Upon each addition of lipid, the cuvette was continuously stirred for at least 4 min before the fluorescence intensity was read to ensure that equilibrium had been established. The total volume added to a sample during the titration was always <5% of the total sample volume. As a control, buffer in the absence of rHFV-C2 was titrated with the same lipid.

Circular Dichroism Measurements. Circular dichroism (CD) spectra were recorded from 250 to 200 nm on an Aviv model 620S spectrometer (Aviv Associates, Inc., Lake Wood, NJ) in a 1 cm path length cell at 24 °C with a bandwidth of 1.0 nm. Data points were collected every 0.5 nm with an average time of 5 s on each point. The digital data were processed, smoothed, and baseline-corrected. For baseline correction, CD spectra of buffer [20 mM KH_2PO_4 and 100 mM NaF (pH 7.4)] containing various concentrations of soluble C6PS were collected. Finally, baseline spectra were subtracted from sample spectra, and the data were converted to molar ellipticity units.

Determination of the Stoichiometry of Phospholipids Binding to rHFV-C2. The stoichiometries of soluble C6PS and C6PC binding to rHFV-C2 were determined by equilibrium dialysis measurements. Experiments were performed using 2.0 mL Teflon dialysis cells (Spectrum Medical) with the two cells separated by an $M_r = 6000-8000$ molecular weight cutoff membrane. The membrane pore was smaller than the protein but larger than the lipid. Initially, one chamber contained 25 μM C6PS (or C6PC) and 5 μM rHFV-C2 (or DTNB-labeled rHFVC-2) while the other chamber contained only 25 μM C6PS (or C6PC). The initial phospholipid concentration was sufficient to saturate >85% of rHFV-C2. The chamber containing rHFV-C2 was allowed to equilibrate with the other chamber at room temperature for 24 h while being rotated horizontally at 20 rpm. The protein concentration gradient between the two halves of the cell causes a difference in the total phosphate concentration between the two halves of the cell. The concentration of protein-bound C6PS (or C6PC) was measured as the difference in total phosphate concentration between the two chambers of the dialysis cell using the inorganic phosphate assay (*3*).

The relationship between the difference in the phosphate concentration in the two halves of the cell and stoichiometry is given as follows

$$\frac{[\Delta L]}{[L]} = \frac{n[P]}{k_d + [L]} \cong \frac{n[P]}{[L]} \qquad (1)$$

where $[\Delta L]$ is the difference in lipid concentration between two chambers, $[L]$ the concentration of phospholipid added to each chamber, $[P]$ the protein concentration present in one half of the chamber, and k_d the equilibrium binding constant. The stoichiometry(s) was calculated from the measured $[\Delta L]/[L]$ value using the second approximate expression. This expression holds when $[L] \gg k_d$, a condition that we were able to generate on the basis of the estimates of k_d made from intrinsic fluorescence titrations as described in the next section.

DATA ANALYSIS

The response of rHFV-C2 intrinsic fluorescence to soluble and membrane lipids was fitted to a binding model described below using a Marquardt−Levenberg weighted, nonlinear least-squares algorithm supplied with Sigmaplot (version 4.2, Jandel Scientific, Corte Madera, CA). Weighting of individual points assumed errors were proportional to the square

Table 1: Binding Parameters Associated with the $rHFV_1$-C2 and $rHFV_2$-C2 Binding to Soluble and Membrane Lipids

lipid	k_d (μM)	ΔR_{sat} (%)[a]	N_m[d]	stoichiometry	N_m
$rHFV_2$-C2					
soluble C6PS at 100 mM salt	2.1 ± 0.1	-50 ± 3	5	0.99 ± 0.2[b]	2
soluble C6PS at 600 mM salt	14.3 ± 0.3	-22 ± 2	2	NM[f]	0
soluble C6PC at 100 mM salt	4.5 ± 0.3	-37 ± 4	2	0.97 ± 0.2[b]	2
soluble C6PC at 600 mM salt	50.0 ± 2	-24 ± 2	2	NM	0
soluble C6PG at 100 mM salt	6.3 ± 0.3	-42 ± 3	1	NM	0
DOPS/DOPC membrane at 100 mM salt	0.17+0.03	$+66 \pm 3$	3	45 ± 3[c]	3
DOPS/DOPC membrane at 600 mM salt	0.43 ± 0.02	$+22 \pm 3$	1	30 ± 7[c]	1
DOPG/DOPC membrane at 100 mM salt	0.39 ± 0.03	$+21 \pm 2$	1	42 ± 6[c]	1
DOPC membrane at 100 mM salt	ND[e]	ND	2	NM	0
DTNB-labeled $rHFV_2$-C2					
soluble C6PS at 100 mM salt	ND	ND	2	0.04	1
soluble C6PC at 100 mM salt	ND	ND	1	NM	0
DOPS/DOPC membrane (20:80) at 100 mM salt	0.41 ± 0.01	$+20 \pm 1$	2	30 ± 4[c]	2
$rHFV_1$-C2					
soluble C6PS at 100 mM salt	4.7 ± 0.9	-13 ± 2	2	0.96 ± 0.2[b]	1
soluble C6PC at 100 mM salt	5.3 ± 0.9	-11 ± 1	2	0.97 ± 0.3[b]	1
DOPS/DOPC membrane at 100 mM salt	0.13 ± 0.08	$+80 \pm 3$	2	50 ± 10[c]	2
DOPC membrane at 100 mM salt	ND	ND	2	NM	0

[a] ΔR_{sat} is the percentage change that is observable at saturation $\{[(R_{sat} - R_0)/R_0] \times 100\}$. [b] Measured using the equilibrium dialysis method (see Methods). [c] Stoichiometry number comes from data fitting described in Methods. [d] N_m is the number of measurements. [e] ND, not detected. [f] NM, not measured.

root of the observable. In our experiments, soluble or membrane lipids were added to 0.2 μM rHFV-C2 in buffer [20 mM KH_2PO_4 and 100 mM NaF (pH 7.4)], and the observed fluorescence response was taken to represent the fraction of protein bound to lipid (*22*).

$$\frac{[P]_b}{[P]_T} = \frac{R_{obs} - R_0}{\Delta R_{sat}} \quad (2)$$

where $[P]_b$ and $[P]_T$ are the bound and total protein concentrations, respectively, R_{obs} is the observed fluorescence of the protein in the presence of lipid, ΔR_{sat} ($=R_{sat} - R_0$) is the observed change in fluorescence when all the protein sites are occupied by lipid, and R_0 is the observed response before addition of any lipid.

The observed response is described below in terms of the total concentration of phospholipid added, $[PL]_T$ (*22*).

$$R_{obs} = R_0 + \frac{R_{sat} - R_0}{2[P]_T}([PL]_T/i + [P]_T + k_d) - \frac{R_{sat} - R_0}{2[P]_T}\sqrt{([P]_T + [PL]_T/i + k_d)^2 - (4[P]_T[PL]_T)/i} \quad (3)$$

where k_d is the site dissociation constant and i is the stoichiometry of lipid binding to rHFV-C2. The stoichiometry of soluble C6PS, C6PC, and C6PG binding to rHFV-C2 was initially estimated to be 1:1 to obtain a lower limit of k_d. Using this k_d, we calculated the concentration of C6PS needed to 85% saturate 5 μM rHFV-C2 and used this amount in equilibrium dialysis experiments to obtain an improved estimate of i. The assumption of a 1:1 stoichiometry affects k_d, but the ik_d product remains unchanged as does the calculation of the 85% saturating C6PS concentration. The measured value of i was then used to obtain the final estimate of k_d. The stoichiometry of DOPC/DOPS, DOPC/DOPG, and DOPC membrane binding to rHFV-C2 was taken to be a variable, and the values that best fitted the data are reported in Table 1.

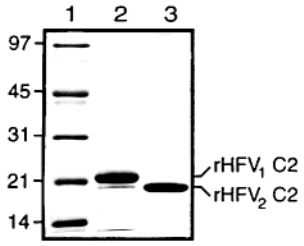

FIGURE 1: SDS−PAGE analysis of rHFV-C2 glycoforms. Samples (10 μg) were electrophoresed on a 15% acrylamide gel and stained with Coomassie blue: MW standards (lane 1), $rHFV_1$-C2 (lane 2), and $rHFV_2$-C2 (lane 3).

RESULTS

Preliminary Characterization of rHFV-C2. The rHFV-C2 construct utilized in these studies encodes the 28-amino acid factor V leader sequence, a five-amino acid peptide linker (AQWYQ), and amino acids 2037−2196 from human factor V. Conditioned medium obtained from insect cell cultures expressing rHFV-C2 typically contained 3−6 μg/mL recombinant protein as determined by an ELISA. Approximately 3 mg of purified rHFV-C2 could be isolated from 1 L of conditioned medium. Analysis of purified rHFV-C2 using SDS−PAGE revealed two peptide bands with apparent molecular masses of 19 and 21 kDa (Figure 1). The 21 kDa species, $rHFV_1$-C2, was eluted in fractions 13−15, whereas the 19 kDa species, $rHFV_2$-C2, was eluted in fractions 15−24. The amino-terminal sequences AQXYQG for $rHFV_1$-C2 and AQWYQGXSTPLGMEN for $rHFV_2$-C2 were identical to the predicted sequence (AQWYQGCSTPLGMEN) of mature rHFV-C2, suggesting that the observed difference in mass was due to alternative glycosylation of Asn^{2181} (*19*). MALDI mass spectrometry of $rHFV_2$-C2 yielded a molecular mass of 19 231 kDa, which is in good agreement with the predicted molecular mass of 19 230.6 kDa. The factor V C2 domain contains one disulfide pair (Cys^{2038}−Cys^{2193}) and one free cysteine (Cys^{2113}) (*28*, *43*). The reactivity of Cys^{2113} in $rHFV_2$-C2 was confirmed by titration with DTNB, which confirmed the presence of one free cysteine residue (data not shown).

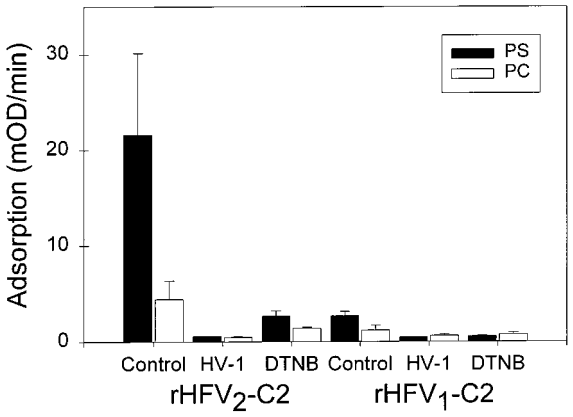

FIGURE 2: Binding of the factor V C2 domain to immobilized phosphatidylserine. Microtiter plate wells were coated with 3 μg/mL rabbit brain PS (black columns) or 3 μg/mL rabbit brain PC (white columns) and blocked with washed buffer. The wells were then incubated with $rHFV_2$-C2 or $rHFV_1$-C2. Binding was detected using the biotinylated antibody 6A5. The binding responses of native recombinant proteins (control), recombinant proteins preincubated with monoclonal antibody HV-1, and recombinant proteins modified by DTNB are shown.

Factor V C2 Domain Binding to Immobilized PS and PC. In previous studies, we used an ELISA to measure the level of C2-dependent binding of factor V and factor V mutants to immobilized PS (*20*, *34*−*36*). In preliminary studies, we confirmed that $rHFV_2$-C2 bound to immobilized PS and that binding was blocked by the monoclonal antibody HV-1, which recognizes amino acids 2037−2087 in the factor V C2 domain (Figure 2). Modification of Cys^{2113} with DTNB also blocked binding of $rHFV_2$-C2 to immobilized PS. The level of binding of $rHFV_2$-C2 to immobilized PC was significantly lower than that observed for immobilized PS, and the observed binding to immobilized PC was also inhibited by both HV-1 and DTNB modification. Glycosylation of Asn^{2181} ($rHFV_1$-C2) also inhibits binding to immobilized PS. Similar to the binding of $rHFV_2$-C2, the binding of $rHFV_1$-C2 to immobilized phospholipid was also inhibited by HV-1 and DTNB modification.

Effect of rHFV-C2 on C6PS Micelle Formation. To use spectroscopic methods to study the interaction of C6PS with rHFV-C2, we had to determine the critical micelle concentration (CMC) of C6PS in the presence of 0.2 μM $rHFV_2$-C2. The aggregate size of soluble C6PS in the presence of $rHFV_2$-C2 was measured with increasing concentrations of C6PS. The variation in average particle size with soluble C6PS concentration is shown in Figure 3. As expected and previously reported for C6PS in the presence of factor X_a (*24*), we could not detect any aggregates at low C6PS concentrations (determination limit of our instrument of ~10 nM) but did detect aggregates once the critical C6PS concentration was reached. Above the CMC, aggregates were always observed, and on the basis of these measurements, the CMC of C6PS was estimated to be 0.1 mM in the presence of 0.2 μM $rHFV_2$-C2. This CMC is 78-fold lower than that observed in the absence of protein (*22*). This is as expected, since the presence of factor X_a has been shown to lower the concentration at which C6PS forms aggregates (*24*).

$rHFV_1$-C2 and $rHFV_2$-C2 Binding to the Soluble C6PS, C6PC, and C6PG and to DOPC/DOPS, DOPC, and DOPC/DOPG Membranes. The binding of $rHFV_1$-C2 and $rHFV_2$-C2 to soluble and membrane phospholipids was studied in a buffer containing 100 mM NaF and 20 mM KH_2PO_4 (pH 7.4). We used NaF instead of NaCl in all experiments to avoid the complication that could arise from chloride ions in circular dichroism experiments. Titration of $rHFV_2$-C2 with C6PS resulted in a 50% decrease in fluorescence at saturating concentrations of C6PS, with a best fit to these data yielding a dissociation constant of 2.1 μM for a stoichiometry of 1:1 [Figure 4A (●) and Table 1]. In contrast, no change in fluorescence was observed when DTNB-modified $rHFV_2$-C2 was titrated with C6PS (○), consistent with our preliminary observation that DTNB modification of Cys^{2113} blocks binding of $rHFV_2$-C2 to immobilized PS.

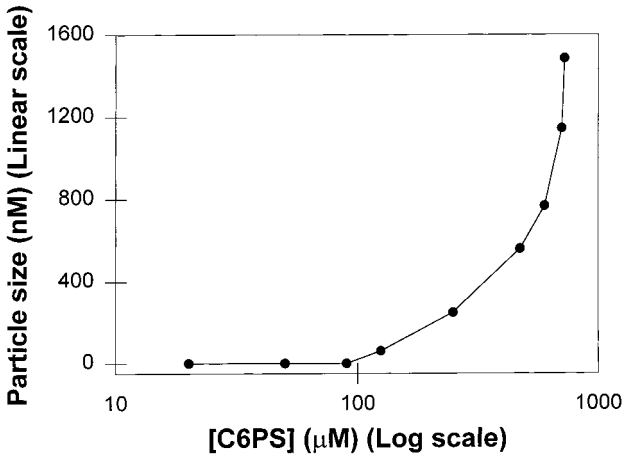

FIGURE 3: Size distribution of C6PS aggregates in the presence of $rHFV_2$-C2 using quasi-elastic light scattering (QELS). The intensity-weighted diameters of C6PS−$rHFV_2$-C2 aggregates in 100 mM NaF and 20 mM KH_2PO_4 (pH 7.4) in the presence of 0.2 μM $rHFV_2$-C2 at various concentrations of C6PS are shown. No aggregates were detected at <0.1 mM C6PS.

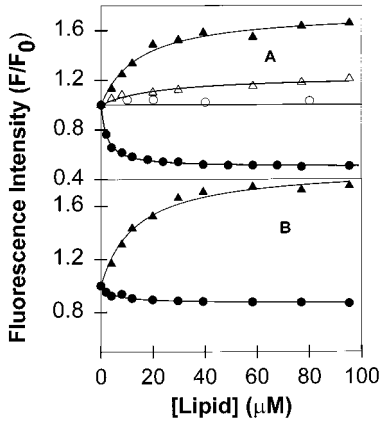

FIGURE 4: (A) Binding of $rHFV_2$-C2 to DOPC/DOPS membranes and soluble C6PS. The intrinsic fluorescence of 0.2 μM $rHFV_2$-C2 was measured in a buffer containing 100 mM NaF and 20 mM KH_2PO_4 (pH 7.4) at 24 °C. Proteins were titrated with DOPC/DOPS (80:20) SUV membranes (▲) and soluble C6PS (●). Data for the titration of DTNB-modified $rHFV_2$-C2 with DOPC/DOPS (80:20) SUV membranes (△) and soluble C6PS are also shown (○). (B) Binding of $rHFV_1$-C2 to DOPC/DOPS membranes and soluble C6PS: The intrinsic fluorescence of 0.2 μM $rHFV_1$-C2 was measured in a buffer containing 100 mM NaF and 20 mM KH_2PO_4 (pH 7.4) at 24 °C. Proteins were titrated with DOPC/DOPS (80:20) SUV membranes (▲) and soluble C6PS (●). Solid lines through the data show the results of fitting the data to eq 3 as discussed in Methods.

Titration of $rHFV_2$-C2 with DOPC/DOPS (80:20) SUV resulted in a 66% increase in the intrinsic fluorescence at saturating lipid concentrations [Figure 4A (▲)]. Regression analysis of these data with eq 3 yielded a dissociation constant of 0.17 μM. DTNB modification reduced the affinity of $rHFV_2$-C2 for DOPC/DOPS (80:20) membranes by 2.4-fold compared to that of the native protein and reduced the relative change in fluorescence observed at saturation [Figure 4A (△)] by 3.3-fold. The $rHFV_1$-C2 glycoform of the C2 domain is glycosylated at Asn^{2181}. Titration of $rHFV_1$-C2 with C6PS resulted in a substantially decreased change in fluorescence [Figure 4B (●)] compared to that of $rHFV_2$-C2. In addition, the regression-derived binding affinity of C6PS for $rHFV_1$-C2 was 2.2-fold weaker than that for $rHFV_2$-C2 (Table 1). In contrast, titration of $rHFV_1$-C2 with DOPC/DOPS (80:20) membranes resulted in an 80% increase in fluorescence at saturating lipid concentrations with an estimated k_d of 0.13 μM [Figure 4B (▲) and Table 1], similar to the results observed for $rHFV_2$-C2. The stoichiometries for membrane binding estimated from regression analysis were similar for $rHFV_1$-C2 and $rHFV_2$-C2 with 45 and 50 phospholipid molecules bound per protein molecule at saturation, respectively.

If we consider the C2 domain to sit as a cylinder with a radius of 10 Å and a height of 38 Å on the membrane surface, we can calculate the stoichiometry to be 8−12, based on the assumption of 70 Å per lipid molecule on the outer leaflet of SUV (*11*). The discrepancy between this estimate and our measured value suggests either that the C2 domain does not occupy the surface at a close packed density at saturation or that the C2 cylinder lies on the membrane surface. Since the expected stoichiometry in the case of completely reclining C2 domains (18−20) would still be lower than the measured value, we must conclude that C2 seems not to pack at optimal packing density on the surface of a membrane. This may be because of clusters of basic residues that line the surface of the protein (*28*). Neither $rHFV_2$-C2 nor $rHFV_1$-C2 bound to membranes containing only DOPC [Figure 5A,B (▲)]. In contrast, both $rHFV_2$-C2 and $rHFV_1$-C2 bound to the soluble phospholipid C6PC with regression-derived dissociation constants only slight larger than those observed for binding to C6PS [Figure 5A,B (●) and Table 1]. Titration of $rHFV_2$-C2 with C6PG resulted in a 42% decrease in fluorescence at saturating concentrations of C6PG, and a best fit to these data yielded a dissociation constant of 6.3 μM for a stoichiometry of 1:1 [Figure 6 (●) and Table 1]. Titration of $rHFV_2$-C2 with DOPC/DOPG (80:20) membranes resulted in a 21% increase in intrinsic fluorescence at saturating lipid concentrations [Figure 6 (▲)]. Regression analysis of these data with eq 3 yielded a dissociation constant of 0.39 μM.

These observations indicate that binding of soluble phospholipid analogues to rHFV-C2 does not show phospholipid headgroup specificity, although binding to a membrane surface did require a negatively charged lipid component. Furthermore, the affinity of $rHFV_1$-C2 and $rHFV_2$-C2 for DOPC/DOPS (80:20) and DOPC/DOPG (80:20) membranes was 10-fold higher than for soluble C6PS, C6PC, or C6PG.

Effect of Ionic Strength on Soluble C6PS, C6PC, and DOPC/DOPS (80:20) Membrane Binding to rHFV-C2. To investigate potential mechanisms for the binding of soluble phospholipid molecules to rHFV-C2, we determined the effect of ionic strength on the affinity of the binding interactions. In the presence of 600 mM NaF, the affinity of $rHFV_2$-C2 for C6PS, C6PC, and DOPC/DOPS (80:20) membranes was decreased approximately 6.8-, 11-, and 2.8-fold, respectively, when compared to values obtained in the presence of 100 mM NaF. These results suggest that electrostatic interactions play a significant role in the binding of C6PS, C6PC, and DOPC/DOPS (80:20) membranes to rHFV-C2.

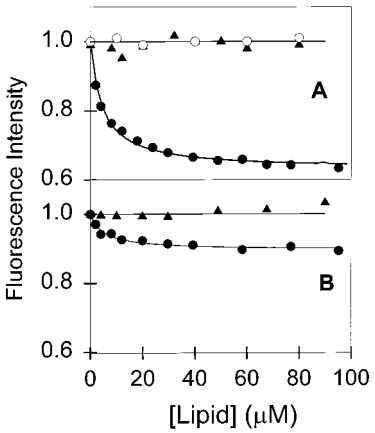

FIGURE 5: (A) Binding of $rHFV_2$-C2 to DOPC membranes and soluble C6PC. The intrinsic fluorescence of 0.2 μM $rHFV_2$-C2 was measured in a buffer containing 100 mM NaF and 20 mM KH_2PO_4 (pH 7.4) at 24 °C. Proteins were titrated with DOPC SUV membranes (▲) and soluble C6PC (●). Data for the titration of DTNB-modified $rHFV_2$-C2 with soluble C6PC are also shown (○). (B) Binding of $rHFV_1$-C2 to DOPC membranes and soluble C6PC. The intrinsic fluorescence of 0.2 μM $rHFV_1$-C2 was measured in a buffer containing 100 mM NaF and 20 mM KH_2PO_4 (pH 7.4) at 24 °C. Proteins were titrated with DOPC SUV membranes (▲) and soluble C6PC (■). Solid lines through the data show the results of fitting the data to eq 3 as discussed in Methods.

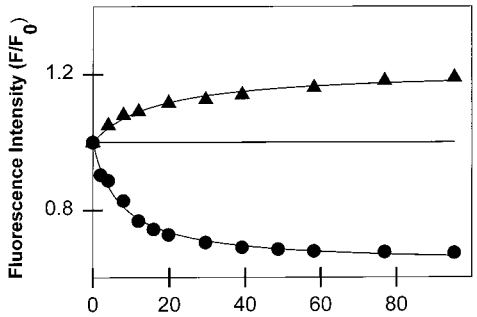

FIGURE 6: Binding of $rHFV_2$-C2 to DOPC/DOPG membranes and soluble C6PG. The intrinsic fluorescence of 0.2 μM $rHFV_2$-C2 was measured in a buffer containing 100 mM NaF and 20 mM KH_2PO_4 (pH 7.4) at 24 °C. Proteins were titrated with DOPC/DOPG (80:20) SUV membranes (▲) and soluble C6PG (●). Solid lines through the data show the results of fitting the data to eq 3 as discussed in Methods.

Stoichiometry of Soluble Phospholipids Binding to the FV C2 Domain. The stoichiometries for the binding of soluble phospholipids to $rHFV_1$-C2 and $rHFV_2$-C2 were determined by equilibrium dialysis as described in Methods. Values calculated with eq 1 are listed in Table 1. Both $rHFV_1$-C2 and $rHFV_2$-C2 bound one molecule of C6PS or C6PC. No binding of C6PS or C6PC to DTNB-modified $rHFV_2$-C2 was detected in equivalent equilibrium dialysis experiments.

Effect of Soluble C6PS on the Secondary Structure of $rHFV_2$-C2. The potential effect of C6PS on the secondary

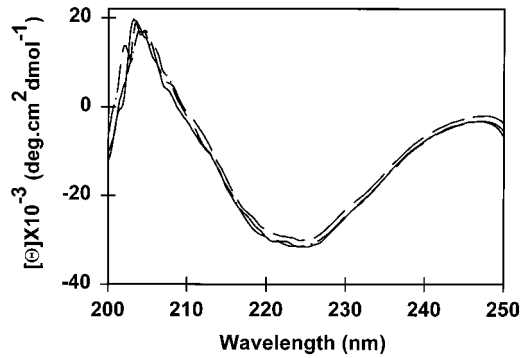

FIGURE 7: Effect of soluble C6PS on the CD spectrum of $rHFV_2$-C2 domain. The CD spectrum of 5 μM $rHFV_2$-C2 in a buffer containing 20 mM KH_2PO_4 and 100 mM NaF (pH 7.4) was recorded at 24 °C in the absence (—), or presence of 25 μM (—·—·—) and 75 μM (— — —) C6PS.

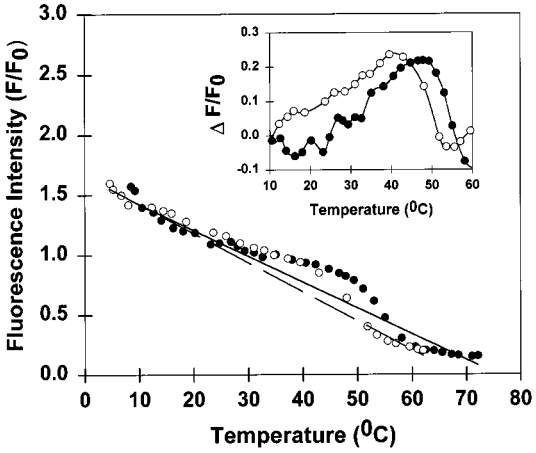

FIGURE 8: Effect of C6PS on the thermal denaturation of $rHFV_2$-C2. The intrinsic fluorescence of 0.2 μM $rHFV_2$-C2 in the buffer containing 100 mM NaF and 20 mM KH_2PO_4 (pH 7.4) was recorded over the temperature range of 5−75 °C. Experiments were performed in the absence (○) or presence (●) of 90 μM C6PS. The dashed (absence) and solid (90 μM C6PS) lines indicate the predicted change in tryptophan fluorescence in the absence of changes in protein conformation. The inset depicts the difference between the observed and expected fluorescence intensity. This difference is expected to reflect thermal denaturation of the C2 domain.

structure of $rHFV_2$-C2 was investigated using circular dichroism (CD) spectroscopy. The CD spectra of 5 μM $rHFV_2$-C2 are shown in Figure 7. Clearly, binding of C6PS to $rHFV_2$-C2 did not result in conformational changes that can be detected by CD spectroscopy.

Thermal Denaturation of $rHFV_2$-C2 in the Presence and Absence of C6PS. We next investigated the effects of C6PS binding on the thermal stability of $rHFV_2$-C2. The thermal denaturation of 0.1 mg/mL $rHFV_2$-C2 was studied using differential scanning calorimetry (DSC). At this protein concentration, we could not detect the thermal melting of $rHFV_2$-C2 over the temperature range of 10−100 °C either in the absence or in the presence of 90 μM C6PS. This could be because $rHFV_2$-C2 could not be denatured in the temperature range or because the enthalpy of the process was too small to detect, since ΔH must be at least 10 times larger than the baseline reproducibility of the DSC scan (~0.8 kcal/mol) to detect denaturation. We next investigated the thermal denaturation of $rHFV_2$-C2 using fluorescence spectroscopy. The fluorescence intensity of 0.2 μM $rHFV_2$-C2 in the absence and presence of 90 μM C6PS was recorded over the temperature range of 5−75 °C (Figure 8). In both cases, the fluorescence intensity decreased in the absence (○) or presence of C6PS (●) with an increase in temperature. The fluorescence of tryptophan residues is expected to decrease linearly with increasing temperature in the absence of structural changes (*21*). The solid and dashed lines represent this expected decrease estimated from the low- and high-temperature regions of the data in the presence and absence of C6PS, respectively. The differences between the observed data and these lines are plotted in the inset of Figure 8. These difference data indicate that $rHFV_2$-C2 undergoes a broad melting transition at 40 °C in the absence of C6PS and at 48 °C in the presence of 90 μM C6PS. Thus, binding of C6PS appears to stabilize the structure of $rHFV_2$-C2.

DISCUSSION

The purpose of this work was to identify the lipid binding site within rHFV-C2 and to shed light on the mechanism by which this domain binds to a PS-containing membrane. The structures of the structurally analogous C2 domains from blood coagulation factors V_a and $VIII_a$ have recently been published (*28*, *38*). On the basis of these structures, it was proposed that membrane binding of these domains also occurs through a hydrophobic residue (Trp in $rHFV_2$-C2) rich patch at the base of the C2 β-sandwich (*28*, *38*). In the case of factor V_a, a rather detailed working model for membrane binding was proposed (*28*). $rHFV_2$-C2 was found to exist in two crystal forms having different conformations (*28*). In an "open" conformation, Trp^{2063}, Trp^{2064}, and Leu^{2116} in the putative membrane-binding region at the β-sandwich base are exposed to water. In a "closed" conformation, these hydrophobic residues cover and are partly buried in a putative PS-specific binding pocked lined with hydrophobic and slightly basic residues (Figure 9). Basic residues adjacent to the pocket are proposed to facilitate approach of the domain to a negatively charged PS-containing membrane and trigger opening of the pocket that is predominantly closed in solution (Figure 9). In the open conformation, Trp^{2063} and Trp^{2064} are proposed to insert into the interface region of the membrane while the PS headgroup occupies the open pocket providing binding specificity. Other PS molecules are thought to interact with basic residues near the pocket to complete the membrane interaction (*28*).

Relation of These Results to the Model for C2 Binding to a Membrane. If it is assumed that DTNB labeling of Cys^{2113} does not alter the structure of the C2 domain, the experiments presented here demonstrate the following:

(1) A single soluble phospholipid binds to rHFV-C2 at a binding site that is blocked by DTNB labeling of Cys^{2113}, which is located at the base of the putative PS-specific binding pocket.

(2) Occupancy of this site is not specific for PS.

(3) Binding of C6PS to $rHFV_2$-C2 occurs without a detectable change in the backbone secondary structure of this domain but with a somewhat increased level of exposure of Trp or Tyr residues to solvent.

(4) Binding of $rHFV_2$-C2 to a PS-containing membrane involves a significantly increased level of protection of Trp or Tyr residues from the solvent, but labeling of Cys^{2113} decreases this extent.

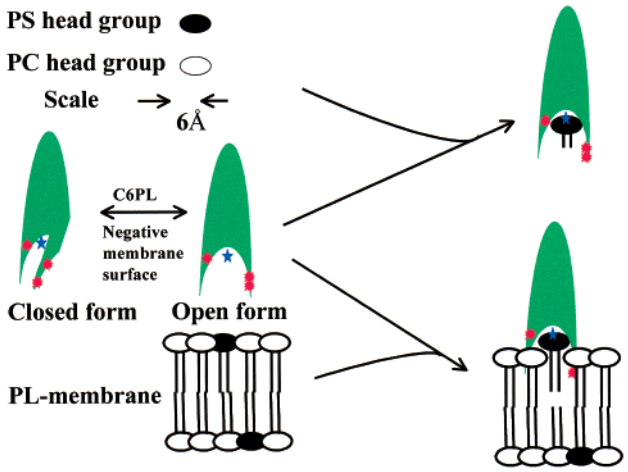

FIGURE 9: Proposed mechanism of soluble lipids and PS-containing membranes binding to the C2 domain. The cartoon represents the binding of rHFV-C2 to soluble lipids and PS-containing membranes. The C2 domain is assumed to exist in two forms, one with its binding pocket open and one with it closed, as suggested by a recently published X-ray structure (*28*). The cartoon is based on the X-ray structure, with the red circles representing the tryptophans (residues 2063, 2064, and 2068) that surround the binding pocket. The blue star represents the Cys^{2113} residue that is labeled by DTNB. We propose that the C2 domain binds to soluble and membrane lipids only in the open conformation. A substantial amount of free energy of binding comes from moving the lipid molecule from water into the hydrophobic binding pocket. Membrane binding is further supported by the free energy releases from the insertion of side chains of the binding pocket to the hydrophobic core of the membrane. Binding of C2 to a membrane is PS-specific due to a small favorable interaction of basic residues in the binding pocket with the acidic PS headgroup. This draws PS out of the bilayer and allows insertion of hydrophobic Trp residues that surround the binding pocket into the membrane interface, an environment known to be favorable to Trp residues. Binding of soluble lipids to C2 is not PS-specific because the major interaction stabilizing the complex is the hydrophobic effect. This strongly suggests that the apparent binding pocket containing Cys^{2113} is the site for PS binding.

(5) Membrane binding requires a negatively charged membrane surface but not necessarily a PS-containing surface.

(6) Glycosylation of $rHFV_2$-C2 at Asn^{2181} had little or no effect on membrane binding but did eliminate the slight preference shown for soluble C6PS over C6PC.

These observations add to and amplify in several ways the previously proposed model for factor V_a C2 domain membrane binding. First, it is clear that the binding pocket is not specific for PS, at least in terms of binding of soluble phospholipids. Only a small contribution to the total free energy of binding is provided by the serine as opposed to the choline (*RT* ln 2.1/4.5 ~ -0.45 kcal/mol; Table 1) or glycerol (~ -0.65 kcal/mol) moiety. The fact that the effect of high salt on the free energy of binding was about the same for C6PS and C6PC (1.2 vs 1.4 kcal/mol; Table 1) implies that the extra negative charge of C6PS was not important in the occupancy of the binding pocket. We conclude that short chain lipid binding is mainly nonspecific and hydrophobic in nature. Nonetheless, occupancy of the binding pocket by different soluble phospholipids elicits different fluorescence responses (Table 1), so it is likely that different phospholipids lead to different structural and potentially different functional responses when the C2 domain is part of whole factor V_a. This could account for some of the well-documented specificity of the prothrombinase for PS (*4*, *13*, *37*). However, it is not clear that factor V_a contributes any of this specificity, which could be due entirely to the PS specificity of factor X_a (*2*, *22*).

Second, not only is occupancy of the binding pocket not specific for PS, but full occupancy of the pocket is not needed for membrane binding. Thus, DTNB labeling of Cys^{2113} did not block membrane binding and caused only a slight increase in the free energy for this process (*RT* ln 0.41/0.17 $\sim$ 0.52 kcal/mol). Nonetheless, DTNB labeling did reduce by a factor of 3 the increase in intrinsic $rHFV_2$-C2 fluorescence associated with membrane binding (Table 1). This suggests that PS occupancy of the binding pocket is necessary for optimal penetration of the membrane by the hydrophobic residues surrounding the binding pocket. On the other hand, DTNB labeling did eliminate binding of soluble C6PS or C6PC. This is consistent with the conclusion reached above that occupancy of the binding pocket by short chain lipids is driven by the favorable free energy of removing the hydrophobic parts of these molecules from water.

Third, it does seem that approach to a negatively charged membrane surface is required for membrane binding (lack of DOPC membrane binding in Figure 5A). This is consistent with the proposal by Macedo-Ribeiro et al. (*28*) that favorable electrostatic contacts favor the open or membrane-binding form of $rHFV_2$-C2. In this form, the burial of Trp^{2063}, Trp^{2064}, and Leu^{2116} in the membrane interface would provide a substantial free energy of binding. Trp has been documented as partitioning strongly to the interface region of membranes (*44*). However, our data show that the required negatively charged surface can be provided by either PS or PG and that occupancy of the putative binding pocket is not specific to PS. These observations do not support the proposal that PS acts specifically as a molecular switch between these two conformations (*28*).

Next, our data suggest that soluble phospholipids can occupy the binding pocket and switch $rHFV_2$-C2 from a closed to an open state. This suggestion is based on the observation that all short chain phospholipid (C6PS, C6PC, or C6PG) binding leads to a decrease in intrinsic fluorescence. We suggest this is because short chain phospholipid binding expels tryptophans from a nonpolar region (presumably the binding pocket) to a region where their fluorescence is quenched by polar water molecules (Figures 4−6). By contrast, the increase in intrinsic fluorescence upon binding to a membrane (e.g., see Figure 4) presumably reflects the insertion of Trp^{2063}, Trp^{2064}, and Trp^{2068} into the membrane interface in the bound state (see Figure 9). The fact that the open and closed states of $rHFV_2$-C2 nearly superimpose throughout their β-sandwich regions (*28*) is also consistent with our observation that the CD spectrum of $rHFV_2$-C2 was unaffected by C6PS binding (Figure 7). But how can the suggestion that even a neutral phospholipid (C6PC) can trigger the closed−open state change be reconciled in terms of the electrostatic switch mechanism described above? To address this, we note that the affinities of C6PS and C6PC binding to rHFV-C2 were all ionic strength-dependent despite the clear implications of our results that binding is dominated by nonspecific hydrophobic effects. Surprisingly, an increase in ionic strength increased the free energy of binding of both

neutral (C6PC) and charged (C6PS) short chain phospholipids by about the same amount (~1.2−1.4 kcal/mol). This suggests that high salt must alter the stability of the open versus the closed state of $rHFV_2$-C2 rather than increase the solubility of the short chain lipids, since the solubility of a neutral and charged lipid should respond differently to ionic strength. An increase in ionic strength also increased the free energy of $rHFV_2$-C2 binding to DOPS/DOPC membranes, but by an amount (~0.55 kcal/mol; Table 1) smaller than that observed for C6PS or C6PC. These effects of high ionic strength are consistent with the possibility that high salt favors the closed (nonbinding) state of C2 but to a lesser extent when C2 is near a charged membrane that presumably favors the open state.

Finally, it remains uncertain whether the switch between these two states has any consequences in terms of the function of factor V_a. However, there are data to suggest that factor V_a undergoes a conformational change as a function of membrane PS content and that membrane PS content does affect function (*37*) in roughly the same way as it affects V_a conformation (*5*).

Effect of Glycosylation on the Membrane Binding of the C2 Domain. Since activation of factor V produces two forms of the light chain, two forms of the activated cofactor appear to exist in plasma, V_{a1} and V_{a2} (*33*, *41*). These result from the presence (V_{a1}) or absence (V_{a2}) of glycosylation at Asn^{2181} in the C2 domain (*19*). Rosing et al. (*39*) have reported that human factor V_{a2} (glycosylated form) binds to PC/PS (80:20) membranes ~45-fold tighter than does factor V_{a1} (nonglycosylated form). On the other hand, our recent studies have shown that both human and bovine factor V_{a2} bind to PC/PS (75:25) membranes with a 3-fold greater affinity than do the human and bovine forms of factor V_{a1} (*19*, *23*). Our current results on the binding of the two forms of rHFV-C2 to PC/PS membranes show that membrane binding of the C2 domain is unaffected by glycosylation (Table 1). If C2 binding is unaffected by glycosylation but whole factor V_a binding affinity is altered by a factor of 3, then glycosylation of C2 must affect some other part of the factor V_a molecule that interacts with membranes. Since rHFV-C2 binds to PC/PS membranes with 50-fold lower affinity than whole factor V_a, the A3 (*14*) or C1 domains of the light chain or the A domains of the heavy chain (*23*) must contribute significantly to factor V_a binding to a membrane. The implication of our results is that glycosylation of Asn^{2181} alters the interaction of the C2 domain with one or more of these other domains in such a way that their interaction with the membrane is impaired.

Comparison of rHFV-C2 Binding to Membranes, Immobilized Lipids, and Soluble Lipids. A common screening assay for the binding of protein to phospholipids is the immobilized PS ELISA illustrated in Figure 2. The observed binding of factor V (*35*) or $rHFV_2$-C2 using this ELISA shows a strong preference for PS over PC, consistent with the requirement of PS for high-affinity binding of factor V to phospholipid vesicles. Surprisingly, we have found in the study presented here that the binding of $rHFV_2$-C2 to the soluble phospholipids C6PS and C6PC does not show headgroup specificity (Table 1 and Figure 5A). In the early phases of our work with the expressed C2 domain, we used the PS ELISA to compare the binding of $rHFV_2$-C2 (unglycosylated form) and $rHFV_1$-C2 (glycosylated form) to immobilized PS. The results (Figure 2) suggested that the glycosylated form of C2 might bind much less tightly to PS than did the unglycosylated form, in agreement with the report of Rosing et al. (*39*). By contrast, our results with PS-containing membranes show no difference in binding affinity between these two forms of the C2 domain (Figure 5 and Table 1). Similarly, in this study, we have found that DTNB modification markedly reduced the level of binding of $rHFV_2$-C2 to immobilized PS or C6PS, while our measurements showed that it had only a small effect on the affinity for binding to DOPS/DOPC membranes. These results illustrate the need to characterize factor V−membrane interactions using membrane bilayers and equilibrium binding assays rather than using soluble phospholipids or phospholipids immobilized on an ELISA plate.

REFERENCES

1. Arai, M., Inaba, H., Higuchi, M., Antonarakis, S. E., Kazazian, H. H., Jr., Fujimaki, M., and Hoyer, L. W. (1989) *Proc. Natl. Acad. Sci. U.S.A. 86*, 4277−81.
2. Banerjee, M., Drummond, D. C., Srivastava, A., Daleke, D., and Lentz, B. R. (manuscript in preparation).
3. Chen, P. S., Toribara, T. Y., and Huber, W. (1956) *Anal. Chem. 28*, 1756−8.
4. Comfurius, P., Smeets, E. F., Willems, G. M., Bevers, E. M., and Zwaal, R. F. (1994) *Biochemistry 33*, 10319−24.
5. Cutsforth, G. A., Koppaka, V., Krishnaswamy, S., Wu, J. R., Mann, K. G., and Lentz, B. R. (1996) *Biophys. J. 70*, 2938−49.
6. Dahlback, B. (1980) *J. Clin. Invest. 66*, 583−91.
7. Davie, E. W., Fujikawa, K., and Kisiel, W. (1991) *Biochemistry 30*, 10363−70.
8. Esmon, C. T. (1979) *J. Biol. Chem. 254*, 964−73.
9. Gill, S. C., and von Hippel, P. H. (1989) *Anal. Biochem. 182*, 319−26.
10. Higgins, D. L., and Mann, K. G. (1983) *J. Biol. Chem. 258*, 6503−8.
11. Huang, C., and Mason, J. T. (1978) *Proc. Natl. Acad. Sci. U.S.A. 75*, 308−10.
12. Jenny, R. J., Pittman, D. D., Toole, J. J., Kriz, R. W., Aldape, R. A., Hewick, R. M., Kaufman, R. J., and Mann, K. G. (1987) *Proc. Natl. Acad. Sci. U.S.A. 84*, 4846−50.
13. Jones, M. E., Griffith, M. J., Monroe, D. M., Roberts, H. R., and Lentz, B. R. (1985) *Biochemistry 24*, 8064−9.
14. Kalafatis, M., Rand, M. D., and Mann, K. G. (1994) *Biochemistry 33*, 486−93.
15. Kane, W. H., and Davie, E. W. (1986) *Proc. Natl. Acad. Sci. U.S.A. 83*, 6800−4.
16. Kane, W. H., and Davie, E. W. (1988) *Blood 71*, 539−55.
17. Kane, W. H., Ichinose, A., Hagen, F. S., and Davie, E. W. (1987) *Biochemistry 26*, 6508−14.
18. Kane, W. H., and Majerus, P. W. (1981) *J. Biol. Chem. 256*, 1002−7.
19. Kim, S. W., Ortel, T. L., Quinn-Allen, M. A., Yoo, L., Worfolk, L., Zhai, X., Lentz, B. R., and Kane, W. H. (1999) *Biochemistry 38*, 11448−54.
20. Kim, S. W., Quinn-Allen, M. A., Camp, J. T., Macedo-Ribeiro, S., Fuentes-Prior, P., Bode, W., and Kane, W. H. (2000) *Biochemistry 39*, 1951−8.
21. Kirby, E. P., and Steiner, R. F. (1970) *J. Phys. Chem. 74*, 4480−90.
22. Koppaka, V., and Lentz, B. R. (1996) *Biophys. J. 70*, 2930−7.
23. Koppaka, V., Talbot, W. F., Zhai, X., and Lentz, B. R. (1997) *Biophys. J. 73*, 2638−52.
24. Koppaka, V., Wang, J., Banerjee, M., and Lentz, B. R. (1996) *Biochemistry 35*, 7482−91.

25. Krishnaswamy, S., and Mann, K. G. (1988) *J. Biol. Chem. 263*, 5714−23.
26. Lee, J., and Lentz, B. R. (1997) *Biochemistry 36*, 421−31.
27. Lentz, B. R., Wu, J. R., Sorrentino, A. M., and Carleton, J. N. (1991) *Biophys. J. 60*, 942−51.
28. Macedo-Ribeiro, S., Bode, W., Huber, R., Quinn-Allen, M. A., Kim, S. W., Ortel, T. L., Bourenkov, G. P., Bartunik, H. D., Stubbs, M. T., Kane, W. H., and Fuentes-Prior, P. (1999) *Nature 402*, 434−9.
29. Mann, K. G., Nesheim, M. E., Church, W. R., Haley, P., and Krishnaswamy, S. (1990) *Blood 76*, 1−16.
30. Monkovic, D. D., and Tracy, P. B. (1990) *J. Biol. Chem. 265*, 17132−40.
31. Nesheim, M. E., Taswell, J. B., and Mann, K. G. (1979) *J. Biol. Chem. 254*, 10952−62.
32. Nicolaes, G. A., Villoutreix, B. O., and Dahlback, B. (1999) *Biochemistry 38*, 13584−91.
33. Odegaard, B., and Mann, K. (1987) *J. Biol. Chem. 262*, 11233−8.
34. Ortel, T. L., Devore-Carter, D., Quinn-Allen, M., and Kane, W. H. (1992) *J. Biol. Chem. 267*, 4189−98.
35. Ortel, T. L., Quinn-Allen, M. A., Charles, L. A., Devore-Carter, D., and Kane, W. H. (1992) *J. Clin. Invest. 90*, 2340−7.
36. Ortel, T. L., Quinn-Allen, M. A., Keller, F. G., Peterson, J. A., Larocca, D., and Kane, W. H. (1994) *J. Biol. Chem. 269*, 15898−905.
37. Pei, G., Powers, D. D., and Lentz, B. R. (1993) *J. Biol. Chem. 268*, 3226−33.
38. Pratt, K. P., Shen, B. W., Takeshima, K., Davie, E. W., Fujikawa, K., and Stoddard, B. L. (1999) *Nature 402*, 439−42.
39. Rosing, J., Bakker, H. M., Christella, M., Thomassen, L. G. D., Hemker, H. C., and Tans, G. (1993) *J. Biol. Chem. 268*, 21130−6.
40. Rosing, J., Tans, G., Govers-Riemslag, J., Zwaal, R., and Hemker, H. (1980) *J. Biol. Chem. 255*, 274−83.
41. Suzuki, K., Dahlback, B., and Stenflo, J. (1982) *J. Biol. Chem. 257*, 6556−64.
42. Villoutreix, B. O., and Dahlback, B. (1998) *Protein Sci. 7*, 1317−25.
43. Xue, J. C., Kalafatis, M., and Mann, K. (1992) *Blood 80*, 162a.
44. Yau, W. M., Wimley, W. C., Gawrisch, K., and White, S. H. (1998) *Biochemistry 37*, 14713−8.

BI010449K